Effect of DC Prestressing on Periodic Grounded DC Tree in Cross-Linked Polyethylene at Different Temperatures

YANI WANG[ID]**, FENG GUO, JIANDONG WU, (Member, IEEE), AND YI YIN, (Member, IEEE)**
Department of Electrical Engineering, School of Electronic Information and Electrical Engineering, Shanghai Jiao Tong University, Shanghai 200240, China
Corresponding author: Yi Yin (yiny@sjtu.edu.cn).

ABSTRACT Periodic grounded dc trees in cross-linked polyethylene under various dc prestressing times are investigated in the temperature range of 20 °C–80 °C. Space charge behaviors in the samples during dc prestressing are simulated based on the bipolar charge transport model. The results reveal that the dc prestressing time has different effects on the tree growth at different temperatures, which is because that the space charge behavior in the sample during dc prestressing is closely related to the dc prestressing time and the temperature, and it has both promotion effect and impedance effect on the tree growth. The moderate promotion effect and impedance effect under 160 s dc prestressing at 20 °C, and the strongest promotion effect and the weakest impedance effect under 240 s dc prestressing at 40 °C result in the largest tree lengths, widths, and accumulated damages under each corresponding condition. At 60 °C and 80 °C, the lengths, widths, and accumulated damages are the largest under 240 s dc prestressing, smaller under 80 s dc prestressing, and the smallest under 160 s dc prestressing, and the reason is believed to be the growth rates reversal during the tree growth. Also it is found that the dc prestressing time has significant effects on the tree shape at 60 °C and 80 °C, which is believed to be related to the wider charge diffusion range under longer dc prestressing time. The electrical tree characteristics are discussed in detail combined with the space charge behaviors.

INDEX TERMS Bipolar charge transport model, dc prestressing, periodic grounded dc tree, space charge, temperature, XLPE.

I. INTRODUCTION

Electrical treeing is an electrically induced crack phenomenon in polymers. Since the electrical trees in polyethylene (PE) under divergent fields were first investigated by the applications of AC voltage, DC voltage, and impulse voltage in 1958 [1], researchers from around the world have made extensive and profound studies on electrical trees in polymers. However, most of the studies were conducted under AC conditions [2]–[7]. In recent years, cross-linked polyethylene (XLPE) DC cables have been used more and more extensively due to the rapid development of high voltage direct current (HVDC) power transmission [8]–[10], so an investigation of electrical trees in XLPE under DC conditions is of great significance.

Although much less reported than those under AC conditions, the characteristics of electrical trees under DC conditions in polymers have been investigated to

some extent. Ieda studied the DC voltage tree, short-circuit tree and polarity reversal tree in PE. It was found that the homocharge injection happened at the needle tip, which induced an electric field distortion [11]. Noto *et al.* [12] studied the electrical trees under DC voltage and impulse voltage in PE, and found that the injected charges from the needle tip reached a steady distribution in microseconds. Sekii *et al.* [13] researched the DC tree and the grounded DC tree in XLPE. The results revealed that the tree inception voltage of the negative DC tree was higher than that of the positive DC tree, whereas that of the negative grounded DC tree was lower than that of the positive grounded DC tree. And these polarity effects were explained by the difference in injected charge amounts between the positive and negative electrodes. Selsjord and Ildstad [14] investigated the electrical tree caused by the rapid DC voltage grounding in XLPE, and found that electrical treeing and breakdown can occur

at an embedded defect as a result of abrupt grounding after DC prestressing at a voltage much lower than the short-term breakdown voltage. The observations were explained by the concept of a field limited space charge injection (FLSC). In a research conducted by Liu and Cao [15] on electrical trees in XLPE under DC voltage, impulse voltage, repetitive DC voltage, and impulse voltage after DC prestressing, the differences among electrical trees under different voltages were explained by the injection, accumulation, dissipation, trapping and detrapping of space charge in the region around the needle tip.

The researches above help us have a certain understanding about the electrical trees under DC conditions in polymers, but they are far from sufficient, and most of them were conducted at room temperature. However, in an HVDC XLPE cable system, the insulation temperature can rise above 70 °C when fully loaded [16]. Hence, XLPE requires further study in relation to a broad temperature range. Besides, during the normal operation of HVDC cable, short circuit fault may occur occasionally, and it has been reported that the electrical tree initiation voltage under this condition is much lower than that under constant DC voltage. Thus an investigation of grounded DC tree is of importance.

Since the electrical trees under DC conditions are closely related to the space charge behaviors, it is necessary to study the space charge characteristics in sample during the treeing experiment. However, the direct measurement of the space charge distribution under the needle-plane electrode system is very difficult, thus the numerical simulation method may be more viable.

In this study, periodic grounded DC trees in XLPE samples under various DC prestressing times were investigated in the temperature range of 20-80 °C. Space charge behaviors in the samples during DC prestressing were simulated based on the bipolar charge transport model. The effects of DC prestressing on the periodic grounded DC tree were discussed combined with the simulation results.

II. EXPERIMENTAL AND SIMULATION METHOD
A. SAMPLE PREPARATION
The XLPE used in this study was a commercial grade HVDC cable insulation material, and the base material is low-density polyethylene (LDPE), antioxidant and crosslinking agent are added. The original LDPE pellets were first mixed at 110 °C for 5 min. After that, the material mixture was thermally pressed at 105 °C for 20 min, and then cross-linked at 180 °C for 15 min at a pressure of 20 MPa. Finally, it was allowed to cool naturally to room temperature under the same pressure. The plate samples were about 110 mm × 15 mm × 5 mm.

The configuration of the sample used for the periodic grounded DC tree experiment is shown in Fig. 1. Ten needles were thermally inserted into the sample using a specially designed device. The needle tip was 3 mm distant from the sample bottom with a radius of 5 μm curvature. Finally, an
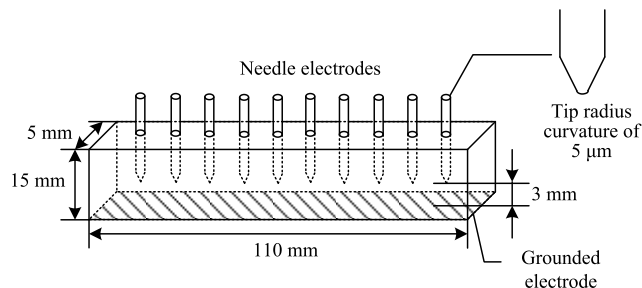
FIGURE 1. Configuration of the sample used for the periodic grounded DC tree experiment.

aluminium plane was attached to the sample bottom to form a needle-plane electrode system. The electric field between two adjacent needle-plane configuration is much lower than that near the needle tip, so the interaction effects between two adjacent needle is ignored here.

To eliminate the possible effect of crosslinking byproducts, all samples were degassed in a vacuum oven under 10^{-2} Pa at 70 °C for 48 h, and then allowed to cool to room temperature at 0.1 °C/min. The degassing results were determined by gas chromatography-mass spectrometry (GC-MS) and not shown here.

B. PERIODIC GROUNDED DC TREE EXPERIMENT
The periodic grounded DC tree experiment system is shown in Fig. 2, which consists of an AC voltage source, a half-wave rectifier, a high voltage relay, a control circuit, a thermometer, a thermostat bath, a sample chamber filled with pure transformer oil and with a sample placed inside. Details of this experiment system can be found in [17].
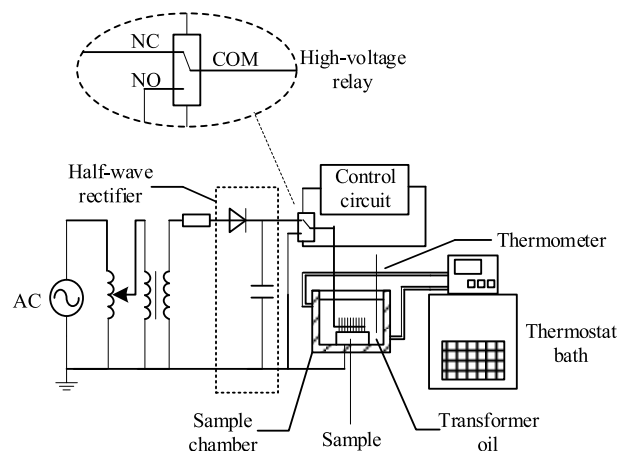
FIGURE 2. Schematic diagram of the periodic grounded DC tree experiment system.

The periodic grounded DC tree experiments were performed under +24 kV at 20, 40, 60, and 80 °C, respectively, by periodic prestressing and grounding. As shown in Fig. 3, the sample was subjected to +24 kV for t_p s, and then grounded for 2 s, a cycle that was repeated for 20 times. At each temperature, experiments were conducted under different DC prestressing times. Considering that it will take
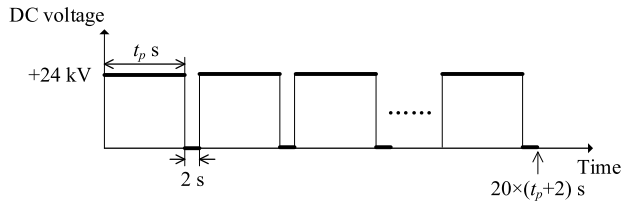
FIGURE 3. Schematic diagram of the periodic grounded DC tree experiment procedure.

some time before the space charge reaches a relatively steady state in the sample, the DC prestressing times were set as 80, 160 and 240 s, respectively. Under each condition, two samples were tested to consider the statistical variations. After the experiment, the sample was cut into 1mm-thick slices along the sides of needles, and observed with the microscope.

C. SIMULATION OF THE SPACE CHARGE BEHAVIOR DURING DC PRESTRESSING

The bipolar charge transport model has been widely used for the simulation of space charge behavior in polymer under the plane-plane electrode system [18]–[21]. It includes charge injection, transport, trapping, detrapping, recombination and extraction. In this paper, this model was applied to the needle-plane electrode system to simulate the space charge behavior in the sample during DC presstressing. The simulation was accomplished with the COMSOL software. In order to reduce the computational complexity and the probability of divergence during the calculating as much as possible, the needle tip was represented as a cone, and the sample was represented as a cylinder. The distance between the needle tip and the sample bottom was 3 mm, which is the same as that in the experiment.

III. EXPERIMENTAL AND SIMULATION RESULTS

A. ELECTRICAL TREE GROWTH

In this study, tree length, width and accumulated damage are adopted to describe the electrical tree growth characteristics. Tree length refers to the maximum distance between the needle tip and the branch tip in the direction of the applied electric field. Tree width refers to the maximum distance between two branch tips in the direction perpendicular to the applied electric field. Accumulated damage is used as a supplement to tree length and width, and it refers to the number of pixel points extracted from the treeing area when it is covered with a fixed size region [22], [23], which is a rectangular region with 603216 pixels here.

Tree lengths under different DC prestressing times at various temperatures are shown in Fig. 4. The tree lengths at different temperatures show different changing trends as the DC prestressing time increases. At 20 °C, the tree lengths under 80 and 240 s DC prestressing are similar, and obviously smaller than those under 160 s DC prestressing. When the temperature rises to 40 °C, the tree lengths under 160 s DC prestressing decrease distinctly, those under 80 s
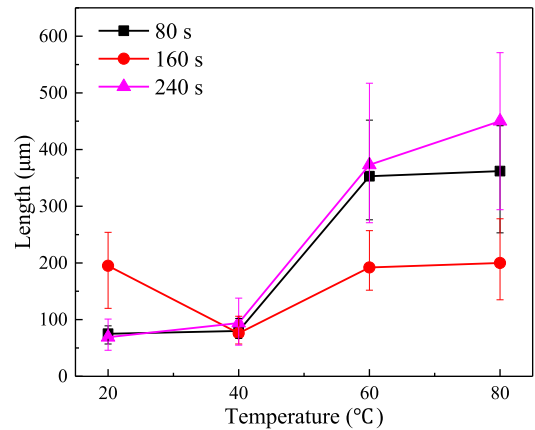
FIGURE 4. Tree lengths under different DC prestressing times at various temperatures.
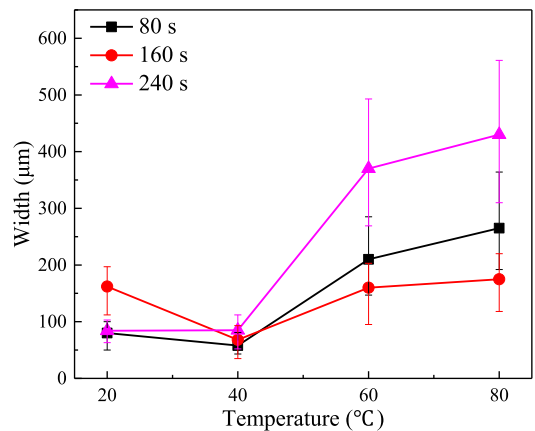
FIGURE 5. Tree widths under different DC prestressing times at various temperatures.

DC prestressing decrease slightly, whereas those under 240 s DC prestressing increase and are slightly larger than the former two. With the further increase of the temperature, tree lengths under three different DC prestressing times all show apparent increasements, and the differences among them are more striking. The tree lengths under 240 s DC prestressing are the largest, those under 80 s DC prestressing are smaller, and those under 160 s DC prestressing are the smallest.

Tree widths under different DC prestressing times at various temperatures are shown in Fig. 5. The changing trends of tree widths are generally similar to those of tree lengths.

Tree accumulated damages under different DC prestressing times at various temperatures are shown in Fig. 6. At 20 °C, the accumulated damages under 160 s DC prestressing are the largest. When the temperature rises to 40 °C, the accumulated damages under 160 s DC prestressing decrease a little, whereas those under the other two DC prestressing times increase a little. The accumulated damages under 240 s are slightly larger than those under 80 and 160 s. When at 60 and 80 °C, all the accumulated damages increase significantly. Those under 240 s DC prestressing are slightly larger
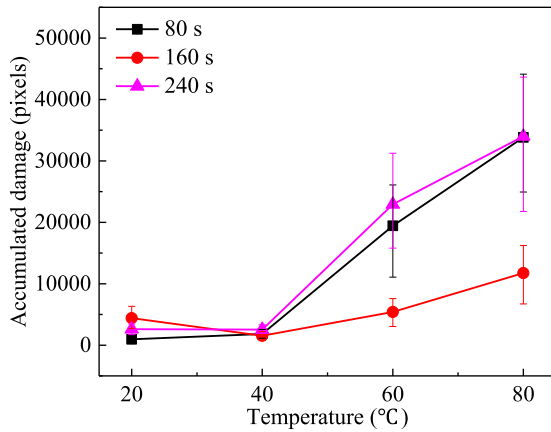
FIGURE 6. Tree accumulated damages under different DC prestressing times at various temperatures.

FIGURE 7. Typical electrical trees under different DC prestressing times at various temperatures.

than those under 80 s DC prestressing, and they both are much larger than those under 160 s DC prestressing.

B. ELECTRICAL TREE SHAPE

Typical electrical trees under different DC prestressing times at various temperatures are shown in Fig. 7. It can be found that although the trees are all branching trees, certain differences are apparent among trees at different temperatures and under different DC prestressing times. When the temperatures are 20 and 40 °C, trees usually have a few thin lateral branches and are narrow as a whole, except that under 160 s DC prestressing at 20 °C. And there is little difference in shape among trees under different DC prestressing times. When the temperatures are 60 and 80 °C, trees have more lateral branches and become thicker in shape. Besides, the differences in shape among trees under different DC prestressing times become significant. When under 80 s DC prestressing, each tree has a long thick branch growing towards the ground electrode, and the lateral branches cross and overlap each other obviously. When under 240 s DC prestressing, each tree has several long thick branches growing towards different directions, making the tree more dispersed in shape, thus less branch cross and overlap is observed. As for the trees under 160 s DC prestressing, although they have more branches compared with those under 160 s at 20 and 40 °C, they are still sparser in shape than those under 80 and 240 s DC prestressing.

Fractal dimension is an effective parameter to describe the tree shape. Usually, the larger the fractal dimension is, the thicker the electrical tree is. To calculate it, the tree is first carefully traced on a blank layer in Photoshop to eliminate the possible effect of the cut traces in the background. And then the new layer is converted into the binary image consisting of series of pixels. After that the binary image is covered with grids of size r, and the minimum number of grids covering the tree is defined as Nr. With the decrease of size r, the fractal dimension, which is represented as FD, can be calculated as [24], [25]:
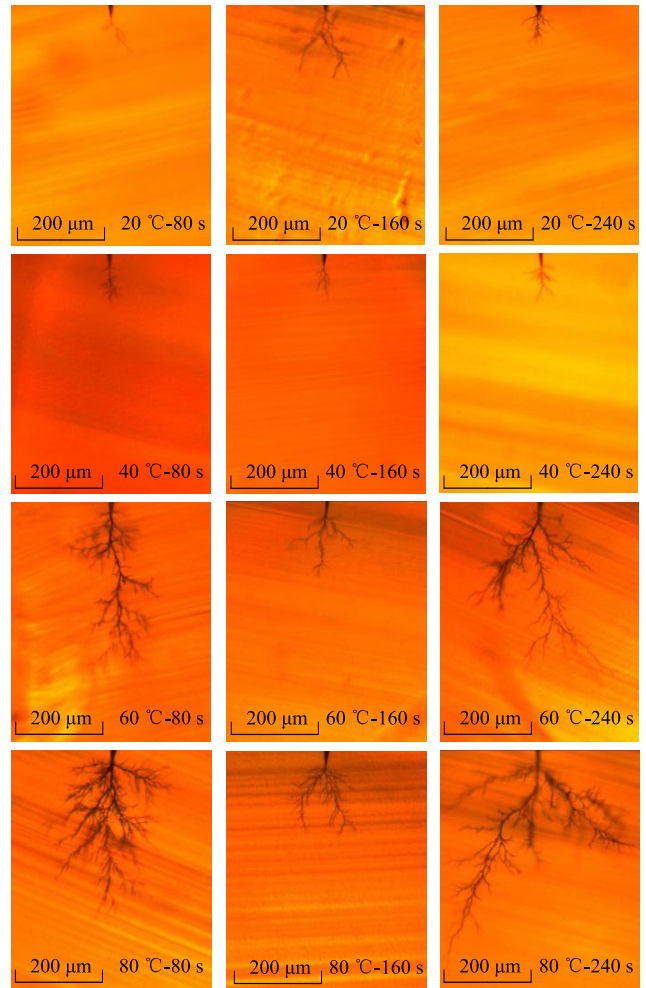
$$FD = \lim \frac{\ln(Nr)}{-\ln(r)} \quad (1)$$

Tree fractal dimensions under different DC prestressing times at various temperatures are shown in Fig. 8. The fractal dimensions under 80 s DC prestressing increase with the temperature monotonically, whereas those under 160 and 240 s DC prestressing decrease as the temperature rises from 20 °C to 40 °C, and then increase as the temperature further rises. When at 20 and 40 °C, the differences in fractal dimension among trees under different DC prestressing times are affected by the grounding time and no obvious regularity is observed, which may be due to the randomness of the electrical tree growth. However, when the temperatures are 60 and 80 °C, the differences become obvious. The fractal dimensions under 80 s DC prestressing are the largest, those under 240 s DC prestressing are smaller, and those under 160 s are the smallest. The calculated fractal dimensions are in good agreement with the tree shapes observed in Fig. 7.
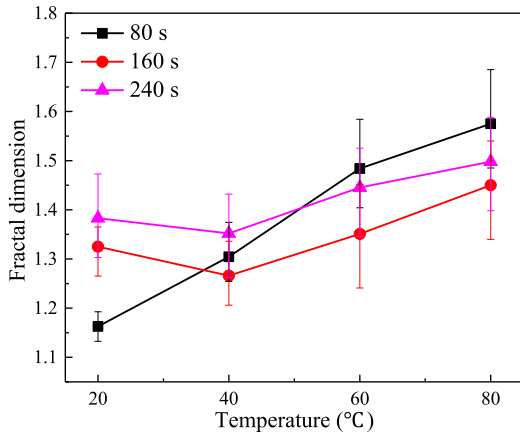
FIGURE 8. Tree fractal dimensions under different DC prestressing times at various temperatures.

TABLE 1. Parameters used for the simulation.

Parameters	Value	Unit
w_{hi}	1.3	eV
w_{ei}	1.27	eV
μ_h	$2\times10^{-6}\exp(-0.54e/kT)$	$m^2 \cdot V^{-1} \cdot s^{-1}$
μ_e	$5\times10^{-6}\exp(-0.54e/kT)$	$m^2 \cdot V^{-1} \cdot s^{-1}$
B_h	0.1	s^{-1}
B_e	0.1	s^{-1}
n_{oht}	100	$C \cdot m^{-3}$
n_{oet}	100	$C \cdot m^{-3}$
S_0, S_1, S_2	4×10^{-3}	$m^3 \cdot C \cdot s^{-1}$
S_3	0	$m^3 \cdot C \cdot s^{-1}$
D_f	$5\times10^{-5}\exp(-0.54e/kT)T$	$m^2 \cdot s^{-1}$
C_h	0.8	1
C_e	0.8	1

C. SPACE CHARGE BEHAVIOR DURING DC PRESTRESSING

In the simulation, the charge injection at the electrodes is described as:

$$\begin{cases} j_h(0,t) = AT^2 \exp\left(-\frac{ew_{hi}}{kT}\right) \exp\left(\frac{e}{kT}\sqrt{\frac{eE(0,t)}{4\pi\varepsilon}}\right) \\ j_e(d,t) = AT^2 \exp\left(-\frac{ew_{ei}}{kT}\right) \exp\left(\frac{e}{kT}\sqrt{\frac{eE(d,t)}{4\pi\varepsilon}}\right) \end{cases} \quad (2)$$

where $j_h(d,t)$ and $j_e(0,t)$ are the extraction current densities for holes at the cathode and electrons at the anode. C_e and C_h are the extraction coefficients for electrons and holes varying from 0 to 1.

The behavior of the charges in the sample can be described as:

$$\begin{cases} j_a(x,t) = \mu_a n_a E(x,t) - D_f \dfrac{dn_a(x,t)}{dx} \\ \dfrac{\partial E(x,t)}{\partial x} = \dfrac{\rho(x,t)}{\varepsilon} \\ \dfrac{\partial n_a(x,t)}{\partial t} + \dfrac{\partial j_a(x,t)}{\partial x} = s_a(x,t) \end{cases} \quad (3)$$

where the subscript a represents the type of the charges, i.e., $h\mu$ and ht for mobile and trapped holes, $e\mu$ and et for mobile and trapped electrons. j_a is the current density. μ_a is the mobility of charges. n_a is the density of charges. D_f is the diffusion coefficient. ρ is the net charge density. s_a is the source term, representing the local change of charge density.

The source terms for holes and electrons can be written as:

$$\begin{cases} s_{ht} = -S_1 \cdot n_{ht}(x) \cdot n_{e\mu}(x) - S_0 \cdot n_{ht}(x) \cdot n_{et}(x) \\ \quad + B_h \cdot n_{h\mu} \cdot \left(1 - \dfrac{n_{ht}(x)}{n_{oht}}\right) - D_h \cdot n_{ht}(x) \\ s_{h\mu} = -S_2 \cdot n_{h\mu}(x) \cdot n_{et}(x) - S_3 \cdot n_{h\mu}(x) \cdot n_{e\mu}(x) \\ \quad - B_h \cdot n_{h\mu} \cdot \left(1 - \dfrac{n_{ht}(x)}{n_{oht}}\right) + D_h \cdot n_{ht}(x) \\ s_{et} = -S_2 \cdot n_{h\mu}(x) \cdot n_{et}(x) - S_0 \cdot n_{ht}(x) \cdot n_{et}(x) \\ \quad + B_e \cdot n_{e\mu} \cdot \left(1 - \dfrac{n_{et}(x)}{n_{oet}}\right) - D_e \cdot n_{et}(x) \\ s_{e\mu} = -S_1 \cdot n_{ht}(x) \cdot n_{e\mu}(x) - S_3 \cdot n_{h\mu}(x) \cdot n_{e\mu}(x) \\ \quad - B_e \cdot n_{e\mu} \cdot \left(1 - \dfrac{n_{et}(x)}{n_{oet}}\right) + D_e \cdot n_{et}(x) \end{cases} \quad (4)$$

where S_i is the recombination coefficient for holes and electrons. B_h and B_e are the trapping coefficients, n_{oht} and n_{oet} are the trap densities, and D_h and D_e are the detrapping coefficients, all for holes and electrons, respectively.

When the holes and the electrons reach the opposite electrodes, they are partially blocked at the interface due to the barriers, which can be described as:

$$\begin{cases} j_h(d,t) = C_h \cdot \mu_h \cdot n_{h\mu}(d,t) \cdot E(d,t) \\ j_e(0,t) = C_e \cdot \mu_e \cdot n_{e\mu}(0,t) \cdot E(0,t) \end{cases} \quad (5)$$

where $j_h(d,t)$ and $j_e(0,t)$ are the extraction current densities for holes at the cathode and electrons at the anode. C_e and C_h are the extraction coefficients for electrons and holes varying from 0 to 1.

The parameterization of the model has been done referring to the values from several previous works [19], [26], [27], and the specific parameters are listed in Table 1.

In the previous research of our lab, the charge mobility μ of the XLPE used in this study was obtained [27], which can be expressed as:

$$\mu = 1.96 \times 10^{-6} \exp\left(-\frac{0.54 \cdot e}{kT}\right) \quad (6)$$

Based on (6), and take the faster movement of electrons than that of the holes as well as the convergence of the simulation into consideration, the μ_h and μ_e in Table 1 are obtained. Besides, according to the Einstein equation, the diffusion coefficient of the charges can be expressed as:

$$D_f = \frac{\mu kT}{e} \quad (7)$$

Thus the D_f can be obtained by plugging (6) into (7), and the calculated D_f is in the range of 10^{-17} to 10^{-15} $m^2 \cdot s^{-1}$. However, during the simulation, it is found

that the calculation is hard to converge with such small D_f, so the D_f in Table 1 is appropriately magnified.

Set the needle tip as the starting point and draw a line perpendicular to the plane electrode. Distributions of the total charges and the trapped holes on the line and near the needle tip at the end of each DC prestressing are shown in Fig. 9. It should be mentioned that this is a result of a single DC prestressing cycle. The origin of the abscissa represents the position of the needle tip. It can be noticed that the total charges near the needle tip are always holes. When the temperature and the DC prestressing time stay the same, the amounts of the total charges are always larger than those of the trapped holes, and they both decrease gradually with the distance until extinction. As the temperature increases, the distribution ranges of the total charges and those of the trapped holes become larger. When at different temperatures, the charge distributions under three different DC prestressing times show obvious differences. At 20 °C, both the amount of the total charges and that of the trapped holes increase with the DC prestressing time. When the temperature rises to 40 °C, charge amounts become larger compared with those at 20 °C. At positions relatively close to the needle tip, the amounts of the trapped holes under 160 and 240 s DC prestressing are very similar, and larger than that under 80 s DC prestressing. As for the amounts of the total charges, those under 80 and 160 s DC prestressing are very similar, and larger than that under 240 s DC prestressing. At positions relatively far from the needle tip, both the amount of the total charges and that of the trapped holes are the largest under 240 s DC prestressing, smaller under 160 s DC prestressing, and the smallest under 80 s DC prestressing. At 60 and 80 °C, the curves of the trapped holes cross with each other, and similar situation can be observed for the curves of the total charges. At positions relatively close to the needle tip, both the amounts of the trapped holes and those of the total charges are the largest under 80 s DC prestressing, smaller under 160 s DC prestressing, and the smallest under 240 s DC prestressing. Whereas at positions relatively far from the needle tip, things become exactly the opposite. In addition, it should be noticed that, compared with those at 60 °C, the amounts of the total charges and those of the trapped holes become smaller at 80 °C, and the differences between them become more significant.

IV. DISCUSSION

A. MECHANISM ANALYSIS OF GROUNDED DC TREE GROWTH

The growth of the grounded DC tree is closely related to the space charge behavior near the needle tip in the sample. During DC prestressing, charges are injected into the material from the needle tip, and some of them get trapped after scattering several times, which is accompanied by the release of energy. The energy is transferred to the electrons in the conduction band, making them hot electrons. These hot electrons may collide with the molecular chains of polymer under the electric field and cause chain scission, which promotes
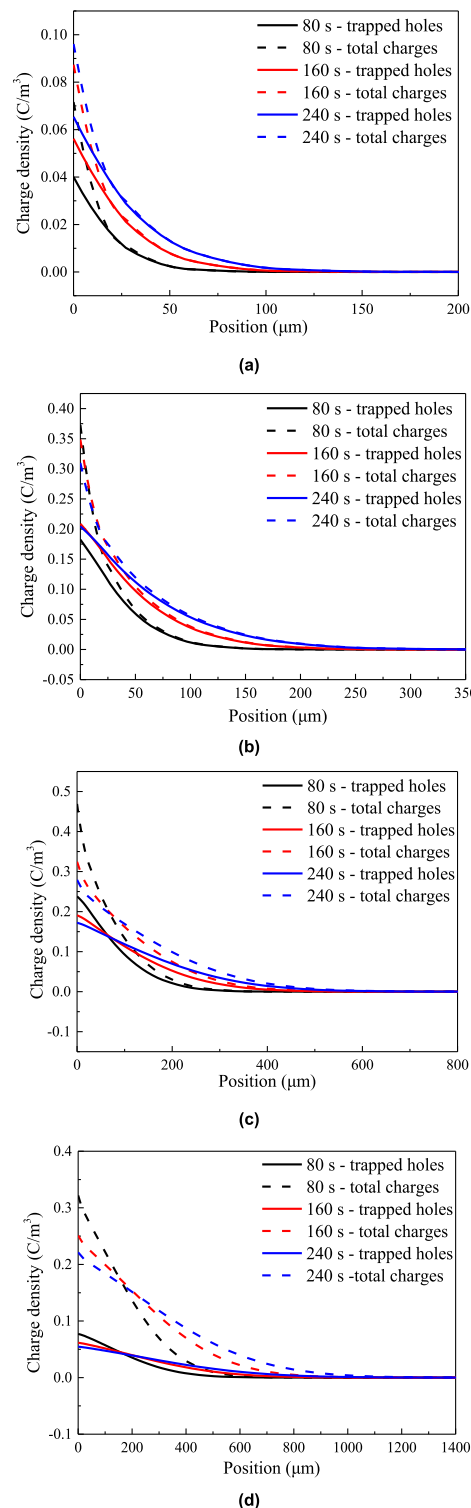
FIGURE 9. Total charges and trapped holes distributions near the needle tip at the end of each DC prestressing at various temperatures. (a) 20 °C. (b) 40 °C. (c) 60 °C. (d) 80 °C.

the electrical tree growth. In the instant of grounding, some trapped charges get detrapped, and the electrical-mechanical energy accumulated around them will be released quickly. If the detrapping time of the charges is less than the dielectric

relaxation time constant of the material, this energy will break the molecular chain and promote the electrical tree growth [28]. Even so, the existence of space charge does not always promote the electrical tree growth. The homocharges accumulated around the needle tip may reduce the electric field, thus the hot electrons will get less energy and cause less damage when colliding with the molecular chains, which impedes the electrical tree growth to some extent.

From what has been discussed above, it can be concluded that the space charge behaviors have both promotion effect and impedance effect on the grounded DC tree growth, which can be indicated by the amount of the trapped holes and that of the total charges near the needle tip, respectively. It is believed that the larger the amount of the trapped holes is, the stronger the promotion effect is. Also, the larger the amount of total charges is, the stronger the impedance effect is. When the promotion effect is stronger than the impedance effect, electrical tree grows.

B. EFFECT OF DC PRESTRESSING ON ELECTRICAL TREE GROWTH AT DIFFERENT TEMPERATURS

From Section 3.1 it can be concluded that the tree lengths, widths, and accumulated damages under 160 s DC prestressing are all larger than those under 80 and 240 s DC prestressing at 20 °C. When the temperature rises to 40 °C, the tree lengths, widths, and accumulated damages under 160 s DC prestressing decrease, whereas those under 240 s DC prestressing increase and are slightly larger than those under 80 and 160 s DC prestressing. At 60 and 80 °C, the tree lengths, widths, and accumulated damages under three different DC prestressing times all increase obviously. And they are the largest under 240 s DC prestressing, smaller under 80 s DC prestressing, and the smallest under 160 s DC prestressing. Those differences in electrical tree growth can be explained combined with the results of space charge simulation.

When at 20 °C, both the amount of the total charges, which indicates the impedance effect of homocharge accumulation, and that of the trapped holes, which indicates the promotion effect of charge trapping and detrapping, increase with the DC prestressing time. It can be inferred that the promotion effect and the impedance effect on electrical tree growth are both the smallest under 80 s DC prestressing, larger under 160 s DC prestressing, and the largest under 240 s DC prestressing. Hence, it may be the moderate promotion effect as well as the moderate impedance effect under 160 s DC prestressing that leads to the largest tree lengths, widths, and accumulated damages. When the temperature rises to 40 °C, at positions relatively close to the needle tip, the amount of the trapped holes under 240 s is similar to that under 160 s DC prestressing and larger than that under 80 s DC prestressing. And the amount of the total charges under 240 s is obviously smaller than those under 80 and 160 s DC prestressing. Thus when under 240 s DC prestressing, the promotion effect is the strongest and the impedance effect is the weakest at positions relatively close to the needle tip.

Considering the small size of trees at 40 °C at the same time, it can be easily understood why the tree lengths, widths, and accumulated damages under 240 s DC prestressing are slightly larger than those under 80 and 160 s DC prestressing. As for the decrease in tree length, width, and accumulated damage under 160 s DC prestressing compared with those at 20 °C, a possible explanation is that both the amount of the trapped holes and that of the total charges under 160 s DC prestressing increase when the temperature rises from 20 °C to 40 °C, but the enhancement of promotion effect is weaker than that of the impedance effect. When at 60 and 80 °C, the curves of the trapped holes cross with each other, and similar situation can be observed for the curves of the total charges. The promotion effect and the impedance effect are both moderate when under 160 s DC prestressing, but the tree length, width, and accumulated damage under 160 s DC prestressing are the smallest compared with those under the other two DC prestressing times, which is quite different from the situation at 20 °C. So it is reasonable to infer that during the electrical tree growth at 60 and 80 °C, it is the promotion effect or the impedance effect that dominates, and tree growth rates reversal occurs. For example, if it is the promotion effect that dominates, then the tree growth rate may be the largest under 80 s DC prestressing, smaller under 160 s DC prestressing, and the smallest under 240 s DC prestressing in the initial phases of electrical tree growth. When the trees develop to a certain length, the tree growth rates reverse and become the largest under 240 s DC prestressing, smaller under 160 s DC prestressing, and the smallest under 80 s DC prestressing. It may be the growth rates reversal that makes the tree length, width, and accumulated damage the largest under 240 s DC prestressing, smaller under 80 s DC prestressing, and the smallest under 160 s DC prestressing.

Besides, it is found from the space charge simulation that the amounts of the total charges and those of the trapped holes become smaller when the temperature rises from 60 °C to 80 °C, and the differences between them become more significant. According to the previous analysis, the promotion effect and the impedance effect at 80 °C should both decrease, and the decrease of the promotion effect should be stronger. However, from the experiments, it is found that the tree lengths, widths and accumulated damages at 80 °C do not become smaller, instead, they are obviously larger than those at 60 °C. This may be due to the strong molecular chain movement and local chain relaxation at 80 °C [17], which leads to the decrease of the electrical mechanical strength of the material. Thus the energy needed for causing molecular chain break becomes less, and electrical tree can develop even when the trapped charges amount becomes much smaller.

C. EFFCET OF DC PRESTRESSING ON ELECTRICAL TREE SHAPE AT DIFFERENT TEMPERATURES

From Section 3.2, it can be concluded that at 20 and 40 °C, trees usually have a few lateral branches. Whereas at 60 and 80 °C, trees have more lateral branches and become

thicker in shape. The tree under 80 s DC prestressing has a long thick branch, and the lateral branches cross and overlap each other obviously. The tree under 240 s DC prestressing has several long thick branches growing towards different directions and is more dispersed in shape. The tree under 160 s DC prestressing is still sparser in shape than those under 80 and 240 s DC prestressing. Those phenomena are in good agreement with the fractal dimensions.

According to (7), the diffusion coefficient of charges increases along with the increase in the mobility of charges and the temperature. Meanwhile, the mobility of charges also get promoted with temperature increasing according to (6). Thus it can be inferred that as the temperature increases, the charge diffusion gets enhanced, and more charges are distributed in the direction perpendicular to the applied electric field, which promotes the growth of lateral branches, making the trees at 60 and 80 °C thicker than those at 20 and 40 °C.

The diffusion of charges is a gradual process, i.e., the longer the DC prestressing time, the wider the charges distributed in the direction perpendicular to the applied electric field. Thus it can be inferred that the charge diffusion ranges under 80 s DC prestressing are smaller than those under 240 s DC prestressing, which leads to the compact shapes and larger fractal dimensions under 80 s DC prestressing, as well as the dispersed shapes and smaller fractal dimensions under 240 s DC prestressing. Compared with the former two, the electrical trees under 160 s DC prestressing show the fewest lateral branches and the smallest fractal dimensions, which is probably due to the restriction of the small size.

V. CONCLUSION

This paper has investigated the effect of DC prestressing on periodic grounded DC tree in XLPE in the temperature range of 20-80 °C. From the experimental and simulation results as well as the discussions presented above, the following conclusions can be drawn.

1) The space charge behavior in the sample is closely related to the DC prestressing time and the temperature. At 20 °C, the amounts of the total charges and the trapped holes both increase with the DC prestressing time. At 40 °C, the amount of the total charges is the smallest and that of the trapped holes is the largest at positions close to the needle tip when under 240 s DC prestressing. At 60 and 80 °C, the curves of the trapped holes under different DC prestressing times cross with each other, and similar situation can be observed for the curves of the total charges.

2) The DC prestressing time has different effects on the tree growth at different temperatures, which is because that the space charge behavior in the sample during DC prestressing has both promotion effect and impedance effect on the tree growth. The moderate promotion effect and impedance effect under 160 s DC prestressing at 20 °C, and the strongest promotion effect and the weakest impedance effect under 240 s

DC prestressing at 40 °C result in the largest tree lengths, widths, and accumulated damages under each corresponding condition. At 60 and 80 °C, the lengths, widths, and accumulated damages are the largest under 240 s DC prestressing, smaller under 80 s DC prestressing, and the smallest under 160 s DC prestressing, and the reason is believed to be the growth rates reversal during the tree growth.

3) The DC prestressing time has significant effects on the tree shape at 60 and 80 °C. Trees under 80 s DC prestressing are thicker than those under 240 s DC prestressing, which is because that the charge diffusion range increases with the DC prestressing time. No obvious change in shape is observed for the trees under 160 s DC prestressing, and it may be due to the restriction of the small size.

REFERENCES

[1] D. W. Kitchin and O. S. Pratt, "Treeing in polyethylene as a prelude to breakdown," *Trans. Amer. Inst. Electr. Eng. III, Power App. Syst.*, vol. 77, no. 3, pp. 180–185, Apr. 1958.
[2] L. A. Dissado, "Understanding electrical trees in solids: From experiment to theory," *IEEE Trans. Dielectr. Electr. Insul.*, vol. 9, no. 4, pp. 483–497, Aug. 2002.
[3] R. Huuva, V. Englund, S. M. Gubanski, and T. Hjertberg, "A versatile method to study electrical treeing in polymeric materials," *IEEE Trans. Dielectr. Electr. Insul.*, vol. 16, no. 1, pp. 171–178, Feb. 2009.
[4] F. Noto and N. Yoshimura, "Voltage and frequency dependence of tree growth in polyethylene," in *Proc. IEEE Conf. Electr. Insul. Dielectr. Phenomena (CEIDP)*, Downingtown, PA, USA, Oct. 1974, pp. 207–217.
[5] R. J. Densley, "An investigation into the growth of electrical trees in XLPE cable insulation," *IEEE Trans. Electr. Insul.*, vol. EI-14, no. 3, pp. 148–158, Jun. 1979.
[6] G. Chen and C. H. Tham, "Electrical treeing characteristics in XLPE power cable insulation in frequency range between 20 and 500 Hz," *IEEE Trans. Dielectr. Electr. Insul.*, vol. 16, no. 1, pp. 179–188, Feb. 2009.
[7] X. Zheng and G. Chen, "Propagation mechanism of electrical tree in XLPE cable insulation by investigating a double electrical tree structure," *IEEE Trans. Dielectr. Electr. Insul.*, vol. 15, no. 3, pp. 800–807, Jun. 2008.
[8] G. Chen, M. Hao, Z. Xu, A. Vaughan, J. Cao, and H. Wang, "Review of high voltage direct current cables," *CSEE J. Power Energy Syst.*, vol. 1, no. 2, pp. 9–21, Jul. 2015.
[9] Y. Murata *et al.*, "Development of high voltage DC-XLPE cable system," *SEI Tech. Rev.*, no. 76, pp. 55–62, Apr. 2013.
[10] H. Ghorbani, M. Jeroense, C.-O. Olsson, and M. Saltzer, "HVDC cable systems—Highlighting extruded technology," *IEEE Trans. Power Del.*, vol. 29, no. 1, pp. 414–421, Feb. 2014.
[11] M. Ieda and M. Nawata, "DC treeing breakdown associated with space charge formation in polyethylene," *IEEE Trans. Electr. Insul.*, vol. EI-12, no. 1, pp. 19–25, Feb. 1977.
[12] F. Noto, N. Yoshimura, and T. Ohta, "Tree initiation in polyethylene by application of DC and impulse voltage," *IEEE Trans. Electr. Insul.*, vol. EI–12, no. 1, pp. 26–30, Feb. 1977.
[13] Y. Sekii, H. Kawanami, M. Saito, K. Sugi, and I. Komatsu, "DC tree and grounded DC tree in XLPE," in *Proc. IEEE Conf. Electr. Insul. Dielectr. Phenomena (CEIDP)*, Nashville, TN, USA, Oct. 2005, pp. 523–526.
[14] M. Selsjord and E. Ildstad, "Electrical treeing caused by rapid DC-voltage grounding of XLPE cable insulation," in *Proc. IEEE Int. Symp. Electr. Insul. (ISEI)*, Toronto, ON, Canada, Jun. 2006, pp. 502–505.
[15] Y. Liu and X. Cao, "Electrical tree initiation in XLPE cable insulation by application of DC and impulse voltage," *IEEE Trans. Dielectr. Electr. Insul.*, vol. 20, no. 5, pp. 1691–1698, Oct. 2013.
[16] L. Lan, J. Wu, Y. Yin, X. Li, and Z. Li, "Effect of temperature on space charge trapping and conduction in cross-linked polyethylene," *IEEE Trans. Dielectr. Electr. Insul.*, vol. 21, no. 4, pp. 1784–1791, Aug. 2014.

[17] Y. Wang, G. Li, J. Wu, and Y. Yin, "Effect of temperature on space charge detrapping and periodic grounded DC tree in cross-linked polyethylene," *IEEE Trans. Dielectr. Electr. Insul.*, vol. 23, no. 6, pp. 3704–3711, Dec. 2016.

[18] S. Li, C. Zhao, D. Min, S. Pan, and Y. Yu, "Simulation of low-energy electron beam irradiated PTFE based on bipolar charge transport model," *IEEE Trans. Dielectr. Electr. Insul.*, vol. 23, no. 5, pp. 3016–3025, Oct. 2016.

[19] L. Lan, J. Wu, Y. Yin, and Q. Zhong, "Investigation on heterocharge accumulation in crosslinked polyethylene: Experiment and simulation," *Jpn. J. Appl. Phys.*, vol. 53, no. 7, p. 071702, Jun. 2014.

[20] D. Min, M. Cho, S. Li, and A. R. Khan, "Charge transport properties of insulators revealed by surface potential decay experiment and bipolar charge transport model with genetic algorithm," *IEEE Trans. Dielectr. Electr. Insul.*, vol. 19, no. 6, pp. 2206–2215, Dec. 2012.

[21] Z. Lv, J. Cao, X. Wang, H. Wang, K. Wu, and L. A. Dissado, "Mechanism of space charge formation in cross linked polyethylene (XLPE) under temperature gradient," *IEEE Trans. Dielectr. Electr. Insul.*, vol. 22, no. 6, pp. 3186–3196, Dec. 2015.

[22] B. X. Du, T. Han, and J. G. Su, "Electrical tree characteristics in silicone rubber under repetitive pulse voltage," *IEEE Trans. Dielectr. Electr. Insul.*, vol. 22, no. 2, pp. 720–727, Apr. 2015.

[23] B. X. Du, M. M. Zhang, T. Han, and L. W. Zhu, "Effect of pulse frequency on tree characteristics in epoxy resin under low temperature," *IEEE Trans. Dielectr. Electr. Insul.*, vol. 23, no. 1, pp. 104–112, Mar. 2016.

[24] K. Kudo, "Fractal analysis of electrical trees," *IEEE Trans. Dielectr. Electr. Insul.*, vol. 5, no. 5, pp. 713–727, Oct. 1998.

[25] M. C. Lanca, J. N. Marat-Mendes, and L. A. Dissado, "The fractal analysis of water trees: An estimate of the fractal dimension," *IEEE Trans. Dielectr. Electr. Insul.*, vol. 8, no. 5, pp. 838–844, Oct. 2001.

[26] J. M. Alison and R. M. Hill, "A model for bipolar charge transport, trapping and recombination in degassed crosslinked polyethene," *J. Phys. D, Appl. Phys.*, vol. 27, no. 6, pp. 1291–1299, 1994.

[27] L. Lan, "Effect of temperature on space charge distribution in polymer insulation," (in Chinese), Ph.D. dissertation, School Electron. Inf. Elect. Eng., Shanghai Jiao Tong Univ., Shanghai, China, 2015.

[28] L. Ziyu, L. Rongsheng, W. Huiming, and L. Wenbin, "Space charges and initiation of electrical trees," *IEEE Trans. Electr. Insul.*, vol. EI-24, no. 1, pp. 83–89, Feb. 1989.

FENG GUO was born in Liaoning, China, in 1994. He received the B.Eng. degree in electrical engineering from Shanghai Jiao Tong University, Shanghai, China, in 2016. He is currently pursuing the M.Eng. degree in electrical engineering from Shanghai Jiao Tong University, Shanghai, China. His interest is dielectric properties of polymeric insulation materials.

JIANDONG WU was born in Jiangsu, China, in 1982. He received the B.Sc. and M.E. degrees in electrical engineering from Southwest Jiao Tong University, Chengdu, China, in 2005 and 2008, respectively, and the Ph. D. degree in high voltage and insulation technology from Shanghai Jiao Tong University, Shanghai, China, in 2012. He was with Shanghai Jiao Tong University. From 2010 to 2011, he was also an Assistant Researcher with the Tanaka's Laboratory, IPS Center of Waseda University. His interest is dielectric properties of polymer nanocomposite and electrical insulation.

YI YIN was born in Jiangsu, China. He received the M.Eng. and Ph.D. degree in electrical engineering from Xi'an Jiao Tong University, Xi'an, China, in 1997 and 2000, respectively.

He was a Post-Doctoral Researcher with Shanghai Jiao Tong University, Shanghai, China, from 2000 to 2002. He is currently a Professor with the Department of Electrical Engineering, School of Electronic Information and Electrical Engineering, Shanghai Jiao Tong University. His main research interests are dielectric properties of polymer composites, high voltage technology, condition monitoring, and diagnosis of HV equipment.

Prof. Yin is an International Advisory Committee Member of 2008 and 2011 International Symposium on Electrical Insulating Materials, a Committee Member of Specialization Committee on Engineering Dielectrics of China Electrotechnical Society, and a Committee Member of Specialization Committee on Electric Materials of Shanghai Society for Electric Engineering.

YANI WANG was born in Shannxi, China, in 1991. She received the B.Eng. degree in electrical engineering from Xi'an Jiao Tong University, Xi'an, China, in 2013. She is currently pursuing the Ph.D. degree in electrical engineering with Shanghai Jiao Tong University, Shanghai, China. Her interest is dielectric properties of polymeric insulation.